Supplementary materials for

Role of Acidity in Acid-Clay Catalysts for the Phosgene-Free Synthesis of Methylene Diphenyl Dicarbamate (MDC)

Pengfei Chen, Junfeng Qian, Qun Chen*, Xuan Dai*, Mingyang He

Jiangsu Key Laboratory of Advanced Catalytic Materials and Technology, Changzhou University, Changzhou 213164, China

Contents

Stoichiometric basis and definitions of conversion, selectivity, and yield.

Under ideal conditions the overall stoichiometry is 2 MPC + 1 HCHO → 1 MDC + 1 H_2O. In all screening runs MPC was charged in excess (MPC/HCHO > 2); therefore, conversions were computed on a formaldehyde-limiting basis. The MPC conversion was defined as

$$X_{MPC}^{(HCHO)} = \frac{n_{MPC,0} - n_{MPC,t}}{2n_{HCHO,0}} \times 100\%,$$

where $n_{MPC,0}$ and $n_{MPC,t}$ are the initial and time-t moles of MPC, and $n_{HCHO,0}$ denotes the CH_2O equivalents charged (for 37 wt.% aqueous formaldehyde: $n_{HCHO,0} = m_{solution} \times 0.37/30.03$; for paraformaldehyde or trioxane, calculated from the depolymerized CH_2O equivalents). The MDC selectivity was defined as

$$S_{MDC} = \frac{n_{MDC}}{\sum n_{organics}} \times 100\%,$$

where $\Sigma n_{organics}$ is the sum of all quantified organic products (water excluded). The reported MDC yield was

$$Y_{MDC} = X_{MPC}^{(HCHO)} \times \frac{S_{MDC}}{100}.$$

For completeness, an HCHO-normalized MDC yield is also quoted as

$$Y_{MDC}^{(HCHO)} = \frac{n_{MDC}}{n_{HCHO,0}} \times 100\%,$$

which is ≤100% by stoichiometry (one mole MDC and one mole H_2O per mole HCHO). All amounts are in moles; GC quantification used an internal standard with multi-level calibration.

Preparation TPA/K10 catalysts.

A series of TPA/K10 catalysts was prepared via a conventional wet-impregnation method. Montmorillonite K10 was pre-dried at 120 °C for 4 h prior to impregnation with an aqueous solution of TPA (calculated on an anhydrous basis). The resulting slurry was stirred at room temperature for 2 h, followed by filtration and three successive washes with deionized water to remove unanchored species. The recovered solids were dried sequentially at 40 °C (4 h), 60 °C (4 h), and 100 °C (8 h), cooled to ambient temperature, and gently ground to a homogeneous powder. By varying the amount of TPA introduced during impregnation, a series of catalysts with ICP-determined TPA loadings of 0.54, 0.68, 0.80, and 0.95 wt% (reported as anhydrous TPA) was obtained (Table S1). Detailed formulation procedures and mass-balance calculations are provided in Supporting Information.

Characterization of catalysts.

The crystalline phases of the prepared materials were identified by X-ray diffraction (XRD) on a Rigaku powered diffraction unit with Cu Kα radiation (λ=1.5402 Å, 40 kV, 300 mA). FTIR spectra of the prepared catalyst were collected on a Nicolet PROTÉGÉ 460 FTIR spectrometer using KBr disks. The inductively coupled plasma-atomic emission spectroscopy (ICP-AES) were carried out for quantitative analysis of metal elements using an Agilent ICPMS 7700. The N_2 adsorption–desorption isotherms were measured on a Micromeritics ASAP2460 at 77 K, and then the specific surface area was calculated by the Brunauer-Emmett-Teller (BET) method using the adsorption data in the relative pressure range from 0.05 to 0.30. The pore size distribution curves were calculated from analysis of the adsorption branch of the isotherm using the Barrett-Joyner-Halenda (BJH) method. Thermogravimetric analysis of samples are completed on ZRY-2P TG-DTG under the air atmosphere, the test temperature was 40~700 °C, and the heating rate was 10 °/min.

Table S1. ICP-OES W contents and calculated TPA loadings (anhydrous equivalent) for TPA/K10 catalysts prepared by wet impregnation.

Entry	W (wt.%)[a]	TPA (wt.%)[b]	Catalyst label[c]
1	0.415	0.54	0.54 wt.% TPA/K10
2	0.521	0.68	0.68 wt.% TPA/K10
3	0.613	0.80	0.80 wt.% TPA/K10
4	0.728	0.95	0.95 wt.% TPA/K10

[a] Determined on washed/dried solids by ICP-OES.

[b] Calculated from W using TPA (wt.%) = W (wt.%) / 0.766; TPA reported as anhydrous equivalent of $H_3PW_{12}O_{40}$.

[c] Labels used throughout the manuscript.

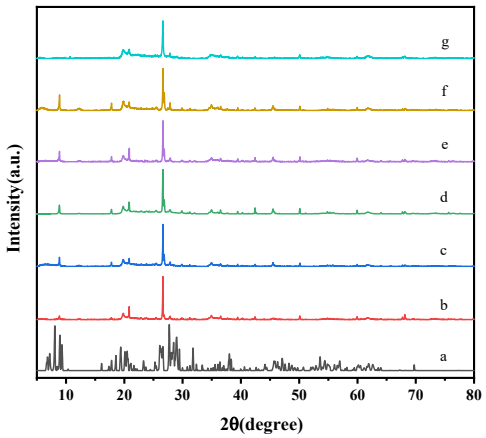

Fig. S1. XRD patterns of (a) bulk TPA, (b) commercial montmorillonite K10 (as received), (c) 0.54 wt% TPA/K10, (d) 0.68 wt% TPA/K10, (e) 0.80 wt% TPA/K10, (f) 0.95 wt% TPA/K10, and (g) acidic clay HM-X.

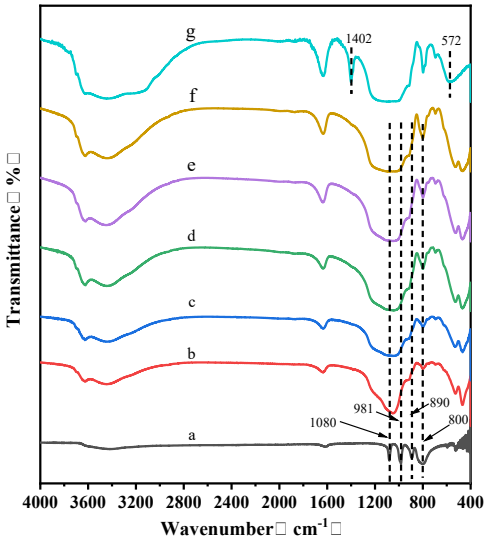

Fig. S2. FTIR spectra of (a) bulk TPA, (b) montmorillonite K10 (as received), (c) 0.54 wt% TPA/K10, (d) 0.68 wt% TPA/K10, (e) 0.80 wt% TPA/K10, (f) 0.95 wt% TPA/K10, and (g) acidic clay HM-X.

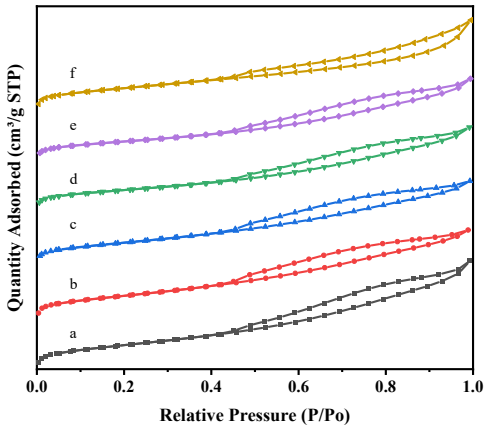

Fig. S3. N_2 adsorption–desorption isotherms of (a) K10, (b) 0.54 wt.% TPA/K10, (c) 0.68 wt.% TPA/K10, (d) 0.80 wt.% TPA/K10, (e) 0.95 wt.% TPA/K10, and (f) acidic clay HM-X.

Table S2. Textural properties of the catalysts from N_2 physisorption.

Entry	Catalyst	$S_{(BET)}$ ($m^2 \cdot g^{-1}$)	V_p ($cm^3 \cdot g^{-1}$)	$D_{(avg)}$ (nm)
1	K10	254.39	0.398	5.113
2	0.54 wt.% TPA/K10	250.43	0.333	5.913
3	0.68 wt.% TPA/K10	220.16	0.304	5.779
4	0.80 wt.% TPA/K10	207.99	0.306	5.902
5	0.95 wt.% TPA/K10	199.44	0.302	5.506
6	HM-X	236.91	0.336	5.675

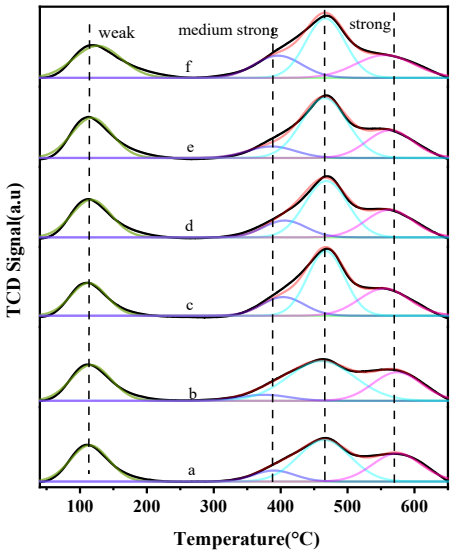

Fig. S4. NH_3-TPD profiles of (a) K10 (as received), (b) 0.54 wt% TPA/K10, (c) 0.68 wt% TPA/K10, (d) 0.80 wt% TPA/K10, (e) 0.95 wt% TPA/K10, and (f) acidic clay HM-X.

Table S3. Integrated peak areas of NH_3-TPD profiles for the catalysts.

Entry	Catalyst	A_w ($mmol \cdot g^{-1}$)	A_m ($mmol \cdot g^{-1}$)	A_s ($mmol \cdot g^{-1}$)	Total ($mmol \cdot g^{-1}$)	Acid density ($mmol \cdot m^{-2}$)
1	K10	2.42	0.79	6.18	9.39	0.037
2	0.54 wt.% TPA/K10	2.52	0.53	7.10	10.16	0.041
3	0.68 wt.% TPA/K10	2.20	1.46	6.99	10.65	0.048
4	0.80 wt.% TPA/K10	2.90	1.40	7.30	11.60	0.056
5	0.95 wt.% TPA/K10	3.11	1.07	7.78	11.96	0.060
6	HM-X	7.99	5.52	19.19	32.70	0.138

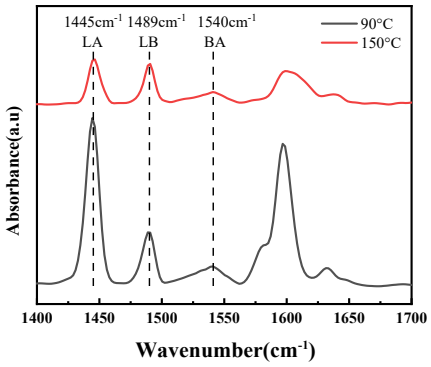

Fig. S5. Pyridine-adsorbed FTIR spectra of the 0.80 wt.% TPA/K10.

Table S4. Distribution of Brønsted and Lewis acid sites of the catalysts.

Catalyst	Temperature (°C)	Brønsted acid area	Lewis acid area	B/L ratio
0.80 wt.% TPA/K10	90	1.266	6.097	0.275
	150	0.720	1.468	0.649
HM-X	90	3.122	9.679	0.427
	150	2.194	3.520	0.825

Catalytic performance of TPA/K10

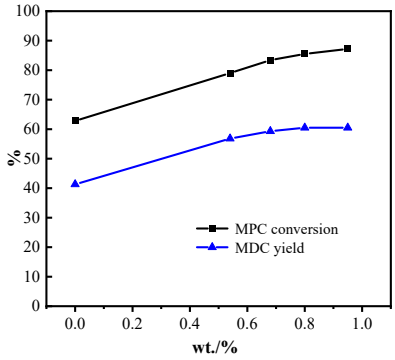

Fig. S6. Effect of TPA loading amount in K10 on MDC conversion and MDC yield. Reaction conditions: MPC 10 mmol; formaldehyde, 37% (w/w) aqueous, *n*(MPC)/*n*(HCHO) = 4; DMC 20 mL; catalyst 1.0 g; 90 °C; 4 h.

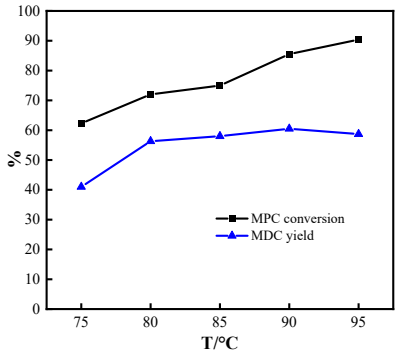

Fig. S7. Effect of reaction temperature on MDC conversion and MDC yield over 0.80 wt% TPA/K10. Reaction conditions: MPC 10 mmol; formaldehyde, 37% (w/w) aqueous, *n*(MPC)/*n*(HCHO) = 4; DMC 20 mL; 0.80 wt% TPA/K10 1.0 g; 4 h.

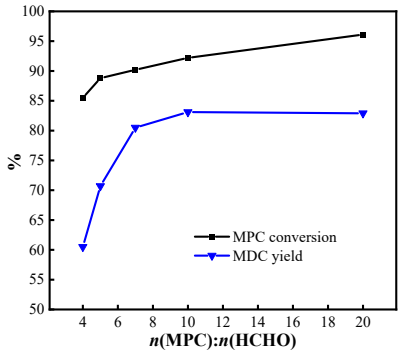

Fig. S8. Effect of the initial molar ratio *n*(MPC)/*n*(HCHO) on MDC formation over 0.80 wt%

TPA/K10.

Reaction conditions: MPC 10 mmol; formaldehyde, 37% (w/w) aqueous; $n(MPC)/n(HCHO) = 4$–20; DMC 20 mL; 0.80 wt% TPA/K10 1.0 g; 90 °C; 4 h.

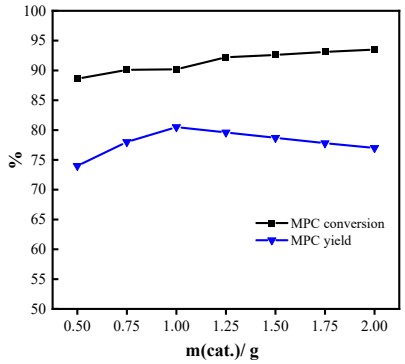

Fig. S9. Effect of catalyst dosage, *m*(cat.), on MDC formation over 0.80 wt% TPA/K10.

Reaction conditions: MPC 10 mmol; formaldehyde, 37% (w/w) aqueous; $n(MPC)/n(HCHO) = 7$; DMC 20 mL; 90 °C; 4 h.

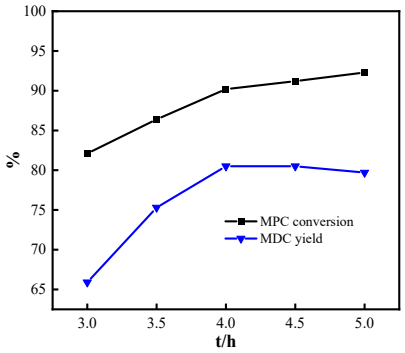

Fig. S10. Effect of reaction time on MDC formation over 0.80 wt% TPA/K10.

Reaction conditions: MPC 10 mmol; formaldehyde, 37% (w/w) aqueous; $n(MPC)/n(HCHO) = 7$; DMC 20 mL; catalyst 1.0 g; 90 °C.

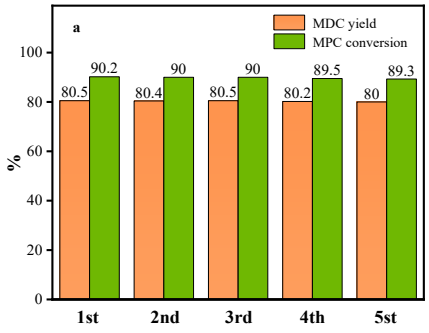

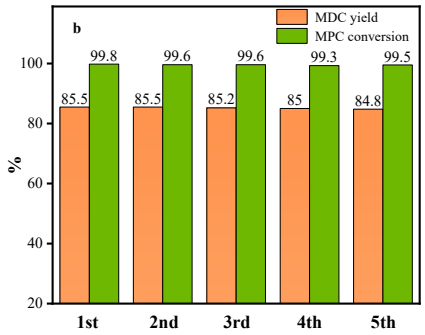

Fig. S11. Catalysts reuse test

Reaction conditions: (a)MPC 10 mmol; formaldehyde, 37% (w/w) aqueous; $n(MPC)/n(HCHO) = 7$; DMC 20 mL; 0.80 wt.% TPA/K10 1.0 g; 90 °C.(b) MPC 10 mmol; formaldehyde, 37% (w/w) aqueous; $n(MPC)/n(HCHO) = 7$; DMC 20 mL; HM-X 1.5 g; $T = 90$℃.

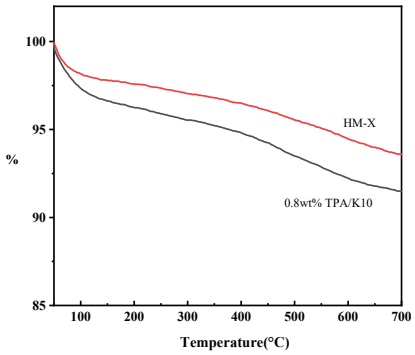

Fig. S12. Thermogravimetric analysis of catalysts.

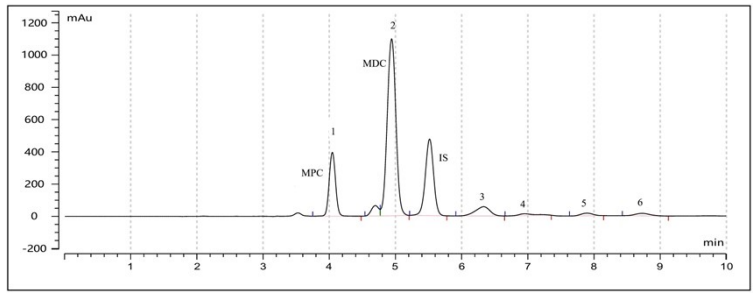

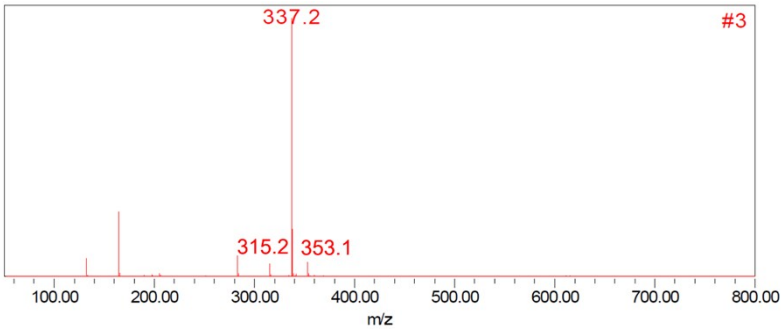

Possible by-products of #3：

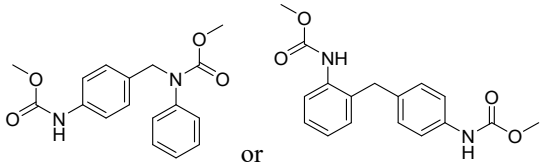

or

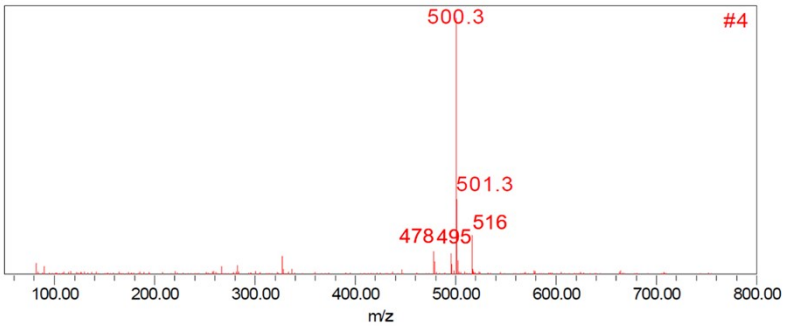

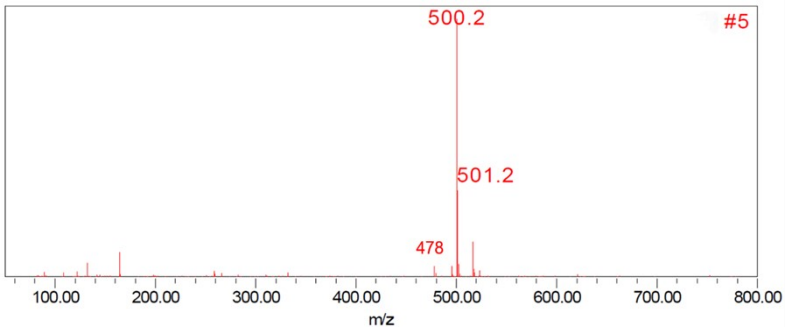

Possible by-products of #4 and #5：

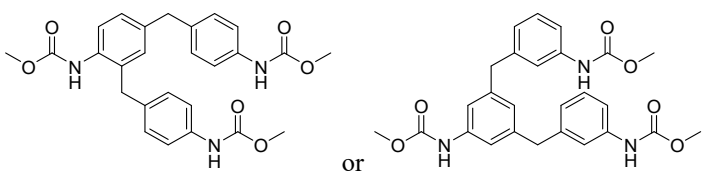

or

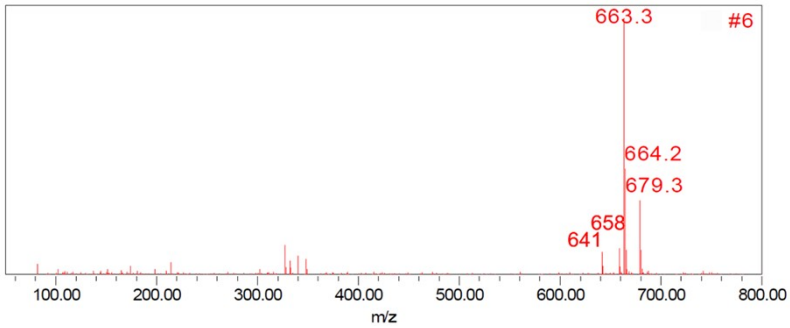

Possible by-product of #6：

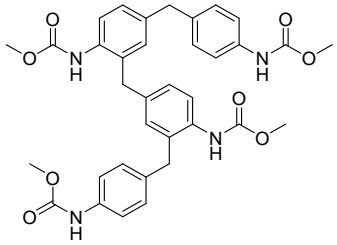

Fig. S13. Liquid chromatogram and mass spectra of the by-products detected in the reaction mixture.